A Review on Position Sensorless Methods for Wind Generators

Soheil Dolatabadi*‡, Sajjad Tohidi**

* Department of Electrical and Computer Engineering, University of Tabriz, 22 Bahman blv., Tabriz, Iran

** Department of Electrical and Computer Engineering, University of Tabriz, 22 Bahman blv., Tabriz, Iran

(s.dolatabadi93@ms.tabrizu.ac.ir, stohidi@tabrizu.ac.ir)

‡ Corresponding Author; Soheil Dolatabadi, s.dolatabadi93@ms.tabrizu.ac.ir

Received: 02.08.2016 Accepted:22.10.2016

Abstract- Wind energy is recognized to be one of the most efficient and effective ways of providing sustainable energy source. Developments in the wind energy area and its lower cost in comparison to other renewable energy sources lead to the fast expansion of wind turbines all over the world. However, there are some concerns about the performance of the off-shore wind turbines where maintenance is too costly. Recently, many research papers come with the ideas how it is possible to eliminate unnecessary parts to reduce the fault probability. Motion sensor is considered to be most attractive part. This paper aims to provide an overview of sensorless control techniques which are used in wind turbines. In this study such methods are divided into machine model, signal injection and artificial intelligent based approaches. The performance of each method, advantages and disadvantages and a brief explanation of methods have been discussed for three types of generators which are double fed induction generators, induction generators and permanent magnet synchronous generators.

Keywords wind turbine; sensorless methods; off-shore wind turbine; speed estimation.

Nomenclature

u, v	voltage	ψ	Flux
I	Current	θ_r	Angle of rotor
V_{sh}	Voltage of High frequency injected signal	Ω	Angular velocity
I_{sh}	Current of High frequency injected signal	P	Pole pair
E	electro motive force	F	frequency
A_s	Stator variable	θ_r	Angle of High frequency signal
A_r	Rotor variable	A_α	Value of A in α axis
A_d	Value of A in direct axis fixed on stator	A_β	Value of A in β axis
A_q	Value of A in quadrature axis fixed on stator	A_s	$\alpha\beta$ Rotational frame with stator velocity
A_D	Value of A in direct axis fixed on rotor	A_r	$\alpha\beta$ Rotational frame with rotor velocity
A_Q	Value of A in quadrature axis fixed on rotor	L	Inductance
A’	Estimated value	R	Resistance

1. Introduction

Environmental issues, especially global warming, have been the target of attention to reduce the greenhouse gas emissions, which are produced mostly due to the electricity generation from fossil fuels. The past decades have witnessed replacement of fossil fuels by renewable sources in several countries. Currently, electricity generated from renewable sources include electricity from solar, wind and ocean wave energy (fuel cells and biomass are excluded due to their gas emissions). Ocean energy is still at the experimental level and has not been commercialized yet. Since the wind turbine (WT) needs lower maintenance and has more efficiency than solar energy (a commercial PV has 10% efficiency at best), it has attracted more attentions. Moreover, wind turbine is able to produce energy with less interruption in comparison to the other renewable resources.

In the past few years, there was a tendency toward off-shore usages in wind turbine applications. For example, Denmark is planning to use wind energy to generate 50% of its electricity consumption by 2030, with turbines which will be placed are off-shore [1]. Using off-shore turbines makes them inaccessible, which requires more money and time for their maintenance in comparison to turbines placed on land. Thus, it is reasonable to reduce the mechanical and electrical parts of turbines as much as possible. Perhaps, one of the most practical choices for elimination is the motion sensor on WT generator. This sensor is used to detect the rotor position/velocity. These measures will then be used in control section to enable the power electronics devices to select an optimized switching pattern. The rotor velocity is necessary for both the wind turbine power generation control and maximum power point tracking (MPPT). Given that 14% of generator failures are directly and 40% of failures are indirectly related to the motion sensors malfunctions, this equipment is crucial in WT. Therefore, researchers have focused on this topic [2], which has resulted in introducing several methods for sensorless motion detection in recent years.

Although sensorless methods are divided into two major groups in many research papers [3, 4], we proposed the following categories for sensorless methods, which are more comprehensive:

1. Sensorless methods based on signal injection: These methods define position of rotor with injecting an external signal. They are known for being very accurate and robust.

2. Sensorless methods based on electrical machine model: Such methods are always accompanied with some assumptions. Besides, using machine equations make these methods dependent on the machine parameters.

3. Sensorless method based on artificial intelligent: This method is completely different from the methods outlined above, as it uses neither external sources nor machine equations. The method defines position/motion by considering previous experiences.

This study aims to explain the most common sensorless methods in three types of generators: permanent magnet synchronous generator (PMSG), doubly fed induction generator (DFIG), and induction generator (IG). The paper then discusses the advantages and disadvantages of each method.

2. Sensorless Methods

2.1. Observer methods

Observer-based sensorless methods use a common structure (Figure 1), which consists of two parts: a real machine and a mathematical model of the machine which is based on the observer equations. The difference between the output signals of the real machine and the modeled machine (here currents are assumed as output) will change the parameters of modeled machine. This process will continue until the difference becomes near to zero. In the subsections below, popular types of this method are presented.

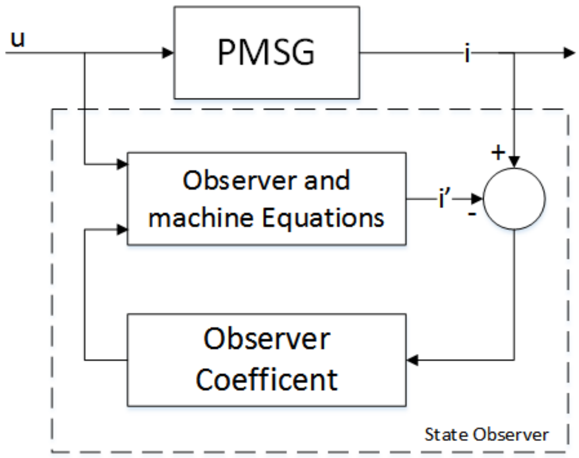

Fig.1. General construction of observation methods [5]

2.1.1. Sliding mode method

Sliding mode method has attracted attention both in industry and academic research [5] due to its simplicity, good accuracy and also robustness against the parameters variation of machine [6-10]. In this method, the output currents are defined by the machine equations according to input voltages. The calculated currents are then subtracted by the measured currents. The result is passed through a sliding controller and it is responsible for revising the model parameters which makes a similar model in comparison to the real machine. The final model is able to compute any variables which are appear in the machine equations. As mentioned before, the method uses sliding controller which has an upper and lower bound. The boundary (±k) is known as sliding mode coefficient.

The outputs of sliding controller in alpha-beta frame are named Z_α and Z_β. Using a low-pass filter, electro motive force (EMF) ($e_{\alpha\beta}$) is estimated as below:

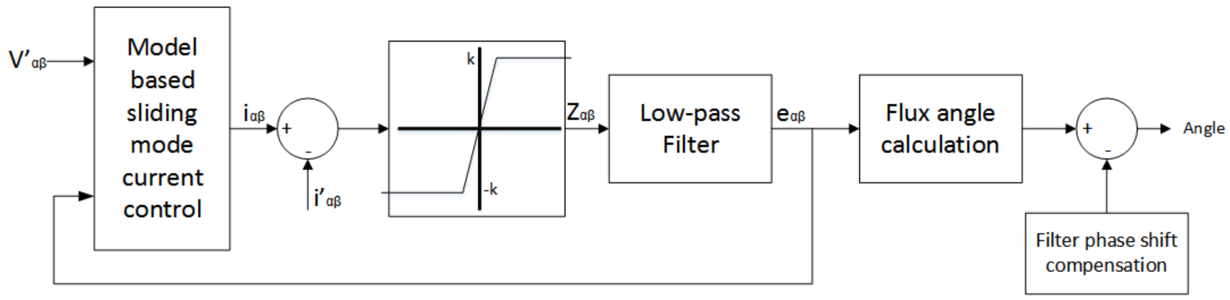

Fig. 2. Block diagram of sliding mode sensorless method [2]

$$\hat{e}_\alpha = \frac{\omega_{cutoff}}{s+\omega_{cutoff}} Z_\alpha$$
$$\hat{e}_\beta = \frac{\omega_{cutoff}}{s+\omega_{cutoff}} Z_\beta \quad (1)$$

From estimated EMF in (1), the rotor position is computed by (2) [2].

$$\theta_r = \tan^{-1}\left(\frac{\hat{e}_\alpha}{\hat{e}_\beta}\right) \quad (2)$$

Figure 2 shows the block diagram of the sliding mode method. Usually, in this method, the current is used as input and rotor position will be the output, but it is impossible to compute the velocity by position derivation due to the noise. In [9, 11], phase lock loop (PLL) has been used to obtain the velocity. Also in [2], model reference adaptive system (MRAS) eliminates the derivation process. In [7], it is stated that the main advantage of using MRAS is its capability to estimate the velocity in the low rotational speeds where majority of sensorless methods are not able to handle this situation. As it could be seen in Figure 2, since this method uses switching (slide block) to define $Z_{\alpha\beta}$, this may produce discrete values with high variations and leads to a noisy output. As mentioned earlier, speed calculation is affected by the noise. Therefore, in [5], a high-order sliding mode observer is proposed to solve this issue. In [12] the author suggests a discreet full-order model which guaranties accuracy of estimation even in twice nominal speed.

2.1.2. Kalman filter method

The general function of Kalman filter [13- 18] is to solve the steady-state dynamic equations which are linear. Since electrical machine equations are non-linear, extended Kalman filter is proposed and used for PMSGs [19]. This method is widely used by researchers in recent years. In [14], the extended method has been proposed for a DFIG. To understand this method better, the relation between the output and input variables should be known. Eq. (3) shows this relation for a DFIG.

$$x_k = f(x_{k-1}.u_{k-1}.w_{k-1})$$
$$y_k = h(x_k.v_k) \quad (3)$$

where f is the dynamic function of the DFIG, h is the output function, v and w are representing system noise and are defined randomly. For DFIG, X_k and u_k are as below:

$$x_k = [i_{sd}\ i_{sq}\ i_{rd}\ i_{rq}\ \theta_r\ T_m]^T \quad (4)$$

$$u_k = [V_{s\alpha}^s\ V_{s\beta}^s\ V_{r\alpha}^r\ V_{r\beta}^r]^T \quad (5)$$

where in Eq.(4) I_{sd}, i_{sq}, i_{rd} and i_{rq} represent stator and rotor currents in direct and quadrature axes, respectively. Two mechanical variables of θ_r and T_m define rotor position and mechanical torque. In Eq.(5), $V_{s\alpha}^s$ and $V_{s\beta}^s$ are stator voltages in α and β frames fixed on stator. Also, $V_{r\alpha}^r$ and $V_{r\beta}^r$ show the stator and rotor voltages in α and β frames fixed on rotor. Using eq. (3) the output will be:

$$y_k = [i_{s\alpha}^s\ i_{s\beta}^s\ i_{r\alpha}^r\ i_{r\beta}^r]^T \quad (6)$$

Assuming that the machine is linear around the operation point and ignoring noises, the Jacobian matrix of H and Φ are obtained as below:

$$\varphi = \frac{\partial f(x.u.0)}{\partial x}$$
$$H = \frac{\partial h(x.0)}{\partial x} \quad (7)$$

Kalman filter algorithm comprises three sections:

I. Initializing algorithm: initial values are defined according to the last value of $X_{0(k-1)}$ and error value (P_{k-1}).

II. Prediction: using the model and last values, prediction is done as below:

$$x_k^- = f(x_{k-1}.u_{k-1})$$
$$P_k^- = \varphi_k|_{x=x^-} P_{k-1}\, \varphi_k^T|_{x=x^-} + Q \quad (8)$$

III. Correction: considering prediction of previous period, below values must be changed:

- Gain of Kalman filter is computed as below:

$$K_k = P_k^- H_k^T|_{x_k^-} \left(H_k|_{x_k^-} P_k^- H_k^T|_{x_k^-} + R\right)^{-1} \quad (9)$$

- Updating x value:

$$x_k = x_k^- + K_k(y_k - h_k(x_k^-.0)) \quad (10)$$

- Calculating rate of deviation:

$$P_k = Pk - K_k H_k\, |x_k\, P_k^- \quad (11)$$

where R and Q represent 'measuring noise' and 'processing noise'.

2.2. Artificial Intelligent method

Artificial neural network (ANN) [20, 21] is trained by feeding the real outputs and inputs. ANN is formed from three layers: input layer, hidden layer and output layer. Each layer contains some neurons and each neuron is connected by a path to another. Number of neurons in output and input is defined by number of input and output variables. Each neuron includes four sections: input, weight and bias, activation function and output. Weight and bias will be defined by training in each iteration of algorithm. In [20], (12) defines how fast the algorithm will be processed:

$$E_n = [i_\alpha . i_\beta . i_\alpha(k-1) . i_\beta(k-1) . v_\alpha . v_\beta] \quad (12)$$

Fig. **3** shows these inputs and outputs and also their connections to the middle layer. To train m[th] neuron, the error should be calculated at first:

$$e_m = d_m - y_m \quad (13)$$

Also, fitness function is defined as (14).

$$E = \frac{1}{2}\sum_m e_m^2 \quad (14)$$

And weight of m[th] neuron is updated by:

$$W(n+1) = w(n) - \eta\left(\frac{\partial E}{\partial w}\right) \quad (15)$$

After training, the rotor velocity can be calculated by giving currents and voltages as inputs and using given weights from training.

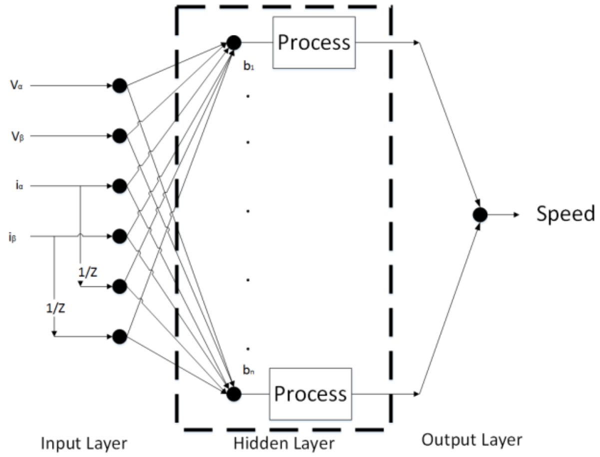

Fig. 3. Structure of ANN [20]

2.3. Phase Lock Loop based methods

Phase Lock Loop (PLL) or frequency lock loop (FLL) based method [22- 30] usually measures 3phase voltages and currents and then computes the quadrature current (i_q) and direct voltage (u_d) by using the Park transformation (abc to dq0). Eq.(16) defines the error between the estimated and real angle by mentioned current and voltage.

$$\Delta\theta_r = -u_d - \omega L_q i_q \quad (16)$$

According to error value, PLL changes the estimated value of rotor speed until error become zero. Fig. **4** depicts the block diagram of PLL based methods.

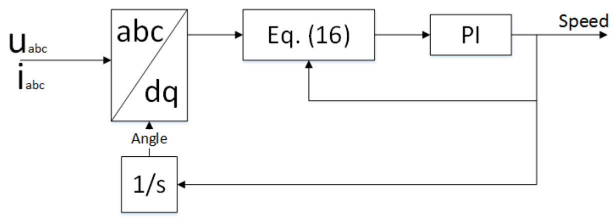

Fig. 4. Structure of PLL based method [31]

It is obvious that equation (16) depends on the machine parameters, so any parameter variations lead to a false answer.

In [31], this problem is solved by online updating of the parameters, but it makes the method more complicated and also expensive. Another major problem occurs when the input voltage is unbalanced, so the estimated speed is absolutely wrong. By using PLL method for the positive sequence of voltage, this problem is eliminated [32].The author proposes a FLL method in [22] which does not use Park transformation, thus the dynamics and accuracy are improved. In [26] a method is presented for IG magnetization which uses PLL method for estimation of rotor flux angle. The method which is presented in [28] does not rely on the machine parameters such as resistance or inductance.

2.4. Flux estimating method

This method [33, 34] uses flux estimator to obtain the rotor angle. The method, which currently has been widely used, has fewer calculations in comparison to the previous ones and has a simple structure. Flux estimating method has two major weaknesses: being unable to respond in low speeds and being sensitive to machine parameter variations. For the most of PMSGs, flux estimator uses the below equations [35]:

$$\psi_{sD} = \int (u_{sD} - R_s i_{sD})dt$$
$$\psi_{sQ} = \int (u_{sQ} - R_s i_{sQ})dt \quad (17)$$

Fig.5 shows its block diagram.

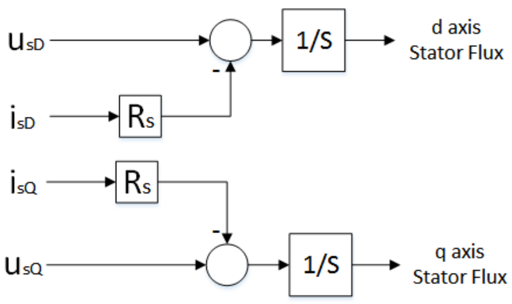

Fig.5. Open loop stator flux observer [35]

Having quadrature and direct stator flux, the rotor angle is computed for a rotational machine by:

$$\theta = \tan^{-1}\frac{\psi_{sD}}{\psi_{sQ}} \quad (18)$$

Although this method has a simple structure, it suffers from pure integral in output which leads to integral drifting error. To solve this problem, closed loop structure is proposed. In this method, stator voltage equation has been rewritten in stator flux rotational frame (Eq.(19)).

$$\overline{u_s} = R_s \overline{i_s} + \frac{d|\bar{\psi}_s|}{dt} + j\omega_{ms}|\bar{\psi}_s| \quad (19)$$

Fig. **6** depicts the block diagrams of the closed loop version. By separating real and imaginary parts, the speed is estimated by using Eq. (20) and Eq. (21).

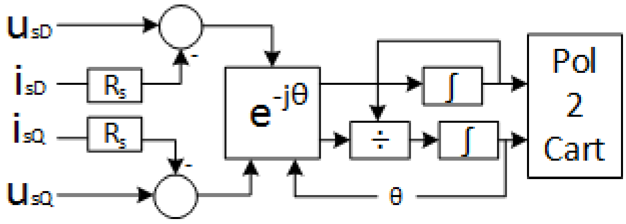

Fig. 6. Control structure of PMLSM with proposed Controller [35]

$$\frac{d|\bar{\psi}_s|}{dt} = u_{sx} - R_s i_{sx} \quad (20)$$

$$\omega_{ms} = \frac{u_{sy} - R_s i_{sy}}{|\bar{\psi}_s|} \quad (21)$$

In [36], by subtracting $L_s i_s$ from stator flux, rotor flux is calculated and the speed can be estimated based on it.

$$\lambda_f = \lambda_s - L_s I_s \quad (22)$$

$$\theta_r = \arctan(\frac{\lambda_{qf}^s}{\lambda_{df}^s}) \quad (23)$$

In [34], the flux observer method was used for DFIG and it was fed with rotor voltages and currents. Fig. **7** shows its block diagram.

$$\lambda_{xm} = \int (v_{xr} - r_r i_{xr})dt - L_r i_{xr}$$
$$\lambda_{ym} = \int (v_{yr} - r_r i_{yr})dt - L_r i_{yr}$$
$$\lambda_m = \sqrt{\lambda_{xm}^2 + \lambda_{ym}^2} \quad (24)$$
$$i_r = \sqrt{i_{xm}^2 + i_{ym}^2}$$

where x and y indices are quadrature and direct axis, respectively. Also, rotor position is defined by equation (25):

$$sin\delta = \frac{\lambda_{ym} i_{xr} - \lambda_{xm} i_{yr}}{\lambda_m i_r} \quad (25)$$

Because the answer is not unique, another equation is necessary.

$$cos\delta = \frac{\lambda_{ym} i_{yr} - \lambda_{xm} i_{xr}}{\lambda_m i_r} \quad (26)$$

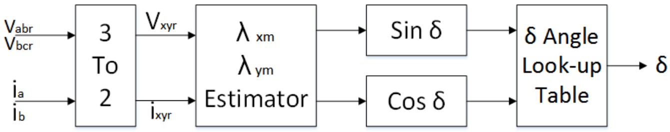

Fig. 7. block diagram of flux estimator method for DFIG [35]

2.5. *EMF method [36, 37]*

Voltage equations of motor are given in below [36]:

$$\begin{cases} E_m = \omega_e \lambda_f \\ v_{qs} = R i_{qs} + L_s\, p\, i_{qs} + \omega_e L_s i_{ds} + E_m \end{cases} \quad (27)$$

Using equation (27) and assuming the motor is not working in flux weakening region (i_{ds}=0), the rotor speed is estimated from Eq.(28).

$$\omega_r = \omega_e = \frac{v_{qs} - R i_{qs} - L_s . p i_{qs}}{\lambda_f} \quad (28)$$

2.6. *MRAS method*

The structure of MRAS method is similar to the observer method. However, the outputs of MRAS are compared with the output of the mathematical model of machine. One of such models does not have speed variable in its equations and is known as reference model. Another model which contains speed variable is named adjustable model. Variables in adjustable model are modified according to the difference between the outputs of adjustable and reference models (see Fig. **8**). When the difference becomes zero, adjustable model is able to estimate the rotor speed.

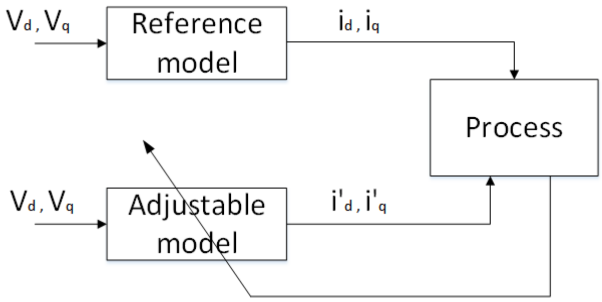

Fig. 8. Block diagram of MRAS method [38]

To obtain adjustable model, mathematical relation of voltage and current for DFIG has been written as below:

$$\frac{d}{dt}\begin{bmatrix} i_d \\ i_q \end{bmatrix} = \begin{bmatrix} -\frac{R_s}{L_d} & \frac{\omega_e L_q}{L_d} \\ -\frac{\omega_e L_d}{L_q} & -\frac{R_s}{L_q} \end{bmatrix} \begin{bmatrix} i_d \\ i_q \end{bmatrix} + \begin{bmatrix} \frac{v_d}{L_d} \\ \frac{v_q - \omega_e \lambda_f}{L_q} \end{bmatrix} \quad (29)$$

Modifying equation (29), it is transformed to **Hata! Başvuru kaynağı bulunamadı.**:

$$\frac{d}{dt}\begin{bmatrix} i_d + \frac{\lambda_f}{L} \\ i_q \end{bmatrix} = \begin{bmatrix} -\frac{R_s}{L_d} & \omega_e \\ -\omega_e & -\frac{R_s}{L_q} \end{bmatrix} \begin{bmatrix} i_d + \frac{\lambda_f}{L} \\ i_q \end{bmatrix} + \begin{bmatrix} \frac{v_d + R_s \lambda_f}{L} \\ \frac{v_q}{L} \end{bmatrix} \quad (30)$$

Then, new voltages and currents are defined as below:

$$\begin{bmatrix} i_d^* \\ i_q^* \\ v_d^* \\ v_q^* \end{bmatrix} = \begin{bmatrix} i_d + \frac{\lambda_f}{L} \\ i_q \\ \frac{v_d + R_s \lambda_f}{L} \\ \frac{v_q}{L} \end{bmatrix} \quad (31)$$

Substituting (31) into **Hata! Başvuru kaynağı bulunamadı.**, the Eq.(32) is obtained :

$$\frac{d}{dt}\begin{bmatrix} i_d^* \\ i_q^* \end{bmatrix} = \begin{bmatrix} -\frac{R_s}{L_d} & \omega_e \\ -\omega_e & -\frac{R_s}{L_q} \end{bmatrix} \begin{bmatrix} i_d^* \\ i_q^* \end{bmatrix} + \begin{bmatrix} v_d^* \\ v_q^* \end{bmatrix} \quad (32)$$

Finally, by substituting estimated values instead of real values, adjustable model will be defined:

$$\frac{d}{dt}\begin{bmatrix}\hat{i}_d\\ \hat{i}_q\end{bmatrix} = \begin{bmatrix}-\frac{\hat{R}_s}{L_d} & \widehat{\omega_e}\\ -\widehat{\omega_e} & -\frac{\hat{R}_s}{L_q}\end{bmatrix}\begin{bmatrix}\hat{i}_d\\ \hat{i}_q\end{bmatrix} + \begin{bmatrix}\hat{v}_d\\ \hat{v}_q\end{bmatrix} \quad (33)$$

The main drawback of this method is its dependency on generator parameters, especially coil resistance, so this issue should be considered. In [39], an adjustable model is proposed which gets the resistance value, which is defined according to coil temperature and current, in addition to the speed input. Also, this method uses a pure integrator which, as mentioned before, leads to drift error. In [40], to solve this problem, the author proposes using the flux-based MRAS and also a high-pass filter is used instead of integrator for flux estimation. The cut-off frequency is defined online by fuzzy algorithm. In reference [38], two MRAS methods, one based on stator flux and another one based on reactive power for DFIG are introduced and compared. Besides, in [41], the miscalculation of machine parameters is discussed as one of the major problems of MRAS. Due to fact that MRAS method is dependent to mutual inductance, In [42] the authors propose a new algorithm for its estimation. In [43] MRAS technique is presented for DFIG which is based on the rotor current and this approach simplifies this method. Hysteresis block is used in [44] instead of PI controller which improves the speed estimation. The MRAS in [45] comes along with many physical modifications, but briefly the loads natural point is connected to midpoint of DC link and the zero sequence load voltage is used for estimation. The standalone DFIG is subjected in [46] where the effects of parameter variation, dynamics and the method accuracy are studied. In [47] the author proposes a novel MRAS method which uses two stator flux models with different structures, the reference model without rotor position and the adjustable model which includes position. An improved MRAS method is proposed in [48] for DFIG during network voltage unbalance. The performance of MRAS on PMSG is studied in [49]. The MRAS method which proposed in [50] uses torque comparison between reference and adaptive model. Although the method has acceptable accuracy, it suffers from dependency on mutual inductance.

A comprehensive comparison is done in [51] among three different types of MRAS: stator flux (SF), rotor current (RC) and reactive power (Q) based for stand-alone DFIG. Both the RC and SF show similar results, but the Q-MRAS shows failure in some situations. Also in [52] another comparison is done between two different structures of MRAS, one with voltage model in parallel with current model and the other one with both the models connected in series. The parallel one shows better performance. Another comparison [53] studies different estimation techniques which including MRAS, which states that although this method is complicated, has better performance.

2.7. High frequency injection method:

This method is one of the most reliable schemes among sensorless methods because of its independency on generator parameters. Also, this method is able to work in any speeds and even it defines rotor position in standstill. This method has been used in two ways [54]:

1. First Injecting high frequency voltage, and then measuring current and extracting high frequency current and then signal processing for estimating the rotor position.
2. First Injecting high frequency current and measuring output voltage, then extracting high frequency voltage and doing signal processing for estimating the rotor position.

Most of the research papers use first method, since number of frame transformation is lower and also has a simpler structure. Although this method is mostly based on the reluctance variation but in [54] it is used for surficial magnet motors and author claims that it works correctly. The author explains that it happens, because there is always a difference between quadrature and direct reluctance.

By injecting high frequency voltage (V_{sh}) with specific frequency (f_{sh}) about 600 Hz, the motor equations in direct-quadrature frame are:

$$V_{sh}\sin(\theta_h-\theta_r) = r_s i_{qsh} + \omega_r(L_d i_{dsh} + \lambda_{PM}) + L_q\frac{di_{qsh}}{dt}$$

$$V_{sh}\cos(\theta_h-\theta_r) = r_s i_{dsh} - \omega_r(L_q i_{qsh}) + L_q\frac{di_{dsh}}{dt} \quad (34)$$

By using equation **Hata! Başvuru kaynağı bulunamadı.**, the injected current (I_{sh}) will be:

$$|I_{sh}|^2 = i_{dsh}^2 + i_{qsh}^2 = R_1(t) + R_2(t) + R_3(t) \quad (35)$$

In [54], it is explained that because the frequency of injected signal is high enough, so just the R_2 term will be remained.

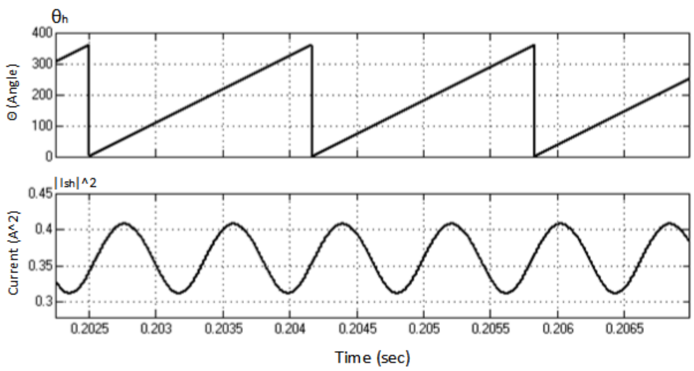

Fig. 9. Output of high frequency method

Due to the rotor reluctance, minimum value of I_{sh} should occur in θ_h=kπ and maximum in θ_h=kπ/2 (k = 1, 3, 5…). Hence if minimum or maximum occurs in another angle, the difference between the angle and expected angle defines the rotor position (figure 9).

This method is widely used for drives of motors in research, but there are some papers about its performance in generator application. In [55], this method is used for DFIG and its results in both the simulation and experimental tests are given. In high frequency injection (HFI) method, other waveforms instead of sinewave could be used, but detection and filtering may become more complicated. HFI method suffers from a major weakness which is nonlinearity of converter because of dead-time in switching. This issue leads to distortion in output voltage and wrong speed calculation. In [56], this problem is eliminated by using a matrix converter. In [57] the authors suggest a new algorithm for PMSG doesn't need any filter for signal extracting or any low-pass filter. Also this approach improves the position estimation by using two opposite voltage vectors. The authors in [58] proposed a method for PMSG to remove the spatial saliency tracking by using injecting three different HF signals, and the method detect magnetic polarity for position estimation. The authors claim that this method has better steady state and dynamic performance compare to conventional HFI methods. The dual three-phase (DTP) PMSM machine is studied for position estimation in [59] where zero-sequence voltage is used for purpose. In [60] the square-wave signal injection method is proposed which uses zero sequence voltage which eliminate the needs of signal amplifying and also simplify signal extraction. The author suggests a method based on induced voltage caused by magnetic saturation which estimates position even in stand still [61]. The all-pass filter is used in [62] to calculate current envelope which this approach causes to better bandwidth and estimate position in half-PWM switching frequency.

2.8. *Combinational methods*

For increasing the efficiency and eliminating weaknesses of sensorless methods, it is reasonable to combine some of these methods to cover each other's weakness. In [63], a combination of sliding-mode and PLL-based methods is proposed for speed estimation. As mentioned, sliding-mode method just defines the rotor position, so a derivate is needed for speed calculation which leads to a noisy answer. Therefore, using a PLL instead of derivative will estimate both speed and rotor position in the same time. In [23], a combination of PLL and flux estimator methods are also used. In [36], flux estimator and EMF methods are used together to increase the dynamic performance, but it leads to an unacceptable response in low speeds. In [64], MRAS and ANN are combined for using in DFIG which is based on rotor current and contrary to [65] it does not depend on machine parameters.

2.9. *New methods*

Few papers have proposed novel sensorless methods which are not welcomed yet and only time could show their successfulness. Some of such methods only make a change in above mentioned methods, and hardly could be considered as novel. In [66], a sensorless method for DFIG is used which defines slip speed based on the comparison between measured and estimated quadrature voltages (Fig. **10**). In [67], a method for rotor slip calculation without Flux estimation is proposed. This method is based on rotor current and estimation of active and reactive power in air gap.

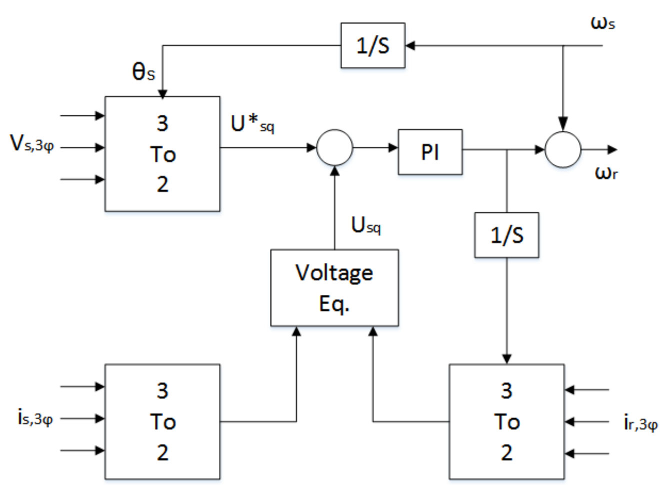

Fig. 10. Block diagram of a new method [66]

3. Effect of MPPT on Sensorless Methods

A common drawback among sensorless methods is their poor performance during low rotor speeds. This issue makes problem for motors drives since the rotor position is required to generate control commands. For example, in direct torque control (DTC) or vector control (VC), the rotor position is always needed even in very low speeds. However, when it comes to generator, it will be different, because the generators are mostly driven according to MPPT [68- 70].

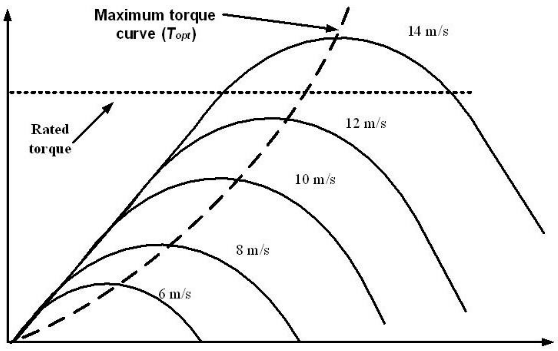

Fig. 11. Output power of generator in different wind speed [68]

As it can be seen in Fig. 11, MPPT just occurs in high rotor speeds, because the output power will be significantly low when rotor speed is low. In addition, mechanical and electrical losses are relatively high, so it leads to low efficiency. Therefore, the power generation is not reasonable and the ganarators will not work in low speed mode and consequently, the failure of sensorless methods in low speeds is acceptable for generators.

4. Conclusion

In this review, a new categorization for sensorless methods is proposed. Then, most of the sensorless methods in papers are introduced and discussed. In this review, it is tangible that although induction generators are very economic, few papers did study on such. In addition, it has been concluded that some methods attracted more attention, such as MRAS and PLL-based. In **Hata! Başvuru kaynağı bulunamadı.**, the number of papers by considering methods and generator types are given. Moreover, in Table 1, the advantages and disadvantages of each method are explained briefly.

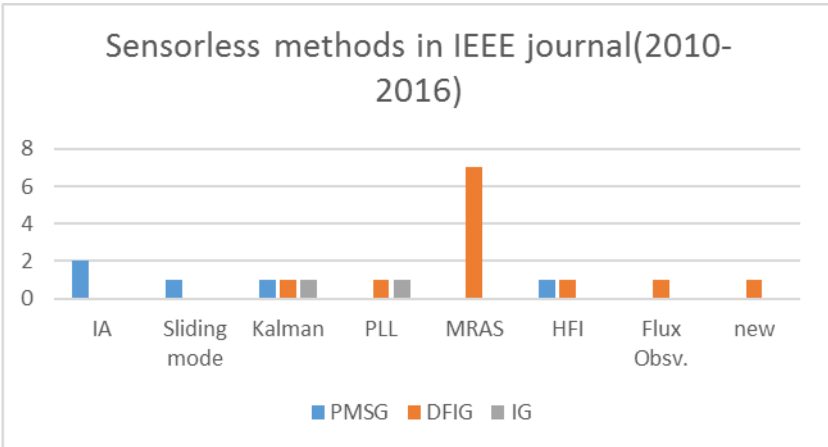

Fig. 12. The number of research papers about sensorless methods in IEEE journals from 2010 to 2016

Table 1. Pros and cons of each method

Method	Pros	Cons	References
PLL based	• Simple structure • High accuracy	• Required high accurate voltage measurement • Depended to motor inductance • Required balanced 3phase voltage	[6, 11, 23, 31]

Sliding mode	• Simple structure • Robustness • Defining rotor position at start	• Required high frequency for sampling (20 KHz) • Just defines position not speed	[6,9]
AI	• Independent from motor parameters • Acceptable response in all speed	• Complexity • High manufacturing and maintaining cost	[20]
MRAS	• Acceptable response in a wide speed range • Doesn't need heavy computing process	• Depended to machine parameters • Required initializing • Drift error in integrator	[43,59]
HFI	• Operation in all speed even standstill	• Increasing electrical losses • Making torque ripple • Producing mechanical noise • complexity	[9,21]
Kalman filter	• high accuracy • acceptable response in low speed • lower approximation	• hard to design and defining gain filter correctly	[9,14]
EMF based	• simplicity • acceptable response in high speed	• due to using inducted voltage as input, wrong answer in low speed • highly depended to machine parameters	[21]
Flux estimator	• simplicity and low calculation	• low accuracy • depended to machine parameters	[33]

References

[1] F. Blaabjerg, Z. Chen and S. Kjaer, "Power electronics as efficient interface in dispersed power generation systems," IEEE Transactions on Power Electronics, vol. 19, no. 5, pp. 1184 - 1194, 2004.

[2] X. Yang, X. Gong and W. Qiao, "Mechanical sensorless maximum power tracking control for direct-drive PMSG wind turbines," in Energy Conversion Congress and Exposition (ECCE), Atlanta, GA, 2010.

[3] J. Holtz, "Sensorless Control of Induction Machines—With or Without Signal Injection?," IEEE Transactions on Industrial Electronics, vol. 53, no. 1, pp. 7 - 30, 2006.

[4] Y.-D. Yoon and S.-K. Sul, "Sensorless Control for Induction Machines Based on Square-Wave Voltage Injection," IEEE Transactions on Power Electronics, vol. 29, no. 7, pp. 3637 - 3645, 2013.

[5] M. Singh and A. Chandra, "Comparative study of sliding mode and ANFIS based observers for speed & position sensor-less control of variable speed PMSG," in 23rd Canadian Conference on Electrical and Computer Engineering (CCECE), Calgary, AB, 2010.

[6] M. Benbouzid, B. Beltran, H. Mangel and A. Mamoune, "A high-order sliding mode observer for sensorless control of DFIG-based wind turbines," in 38th Annual Conference on IEEE Industrial Electronics Society, Montreal, QC, 2012.

[7] K. Huang, L. Zheng, S. Huang and L. Xiao, "Sensorless control for direct-drive PMSG wind turbines based on sliding mode observer," in International Conference on Electrical Machines and Systems (ICEMS), Beijing, 2011.

[8] Z. Xu, P. Ge and D. Xu, "High performance control of a permanent magnet wind power generation system using an adaptive sliding observer," in International Conference on Power Electronics and Drive Systems, 2009. PEDS 2009. , Taipei, 2009.

[9] S. Yang, L. Guo, L. Chang and X. Zhang, "Closed-loop control on PMSG torque in direct-drive wind power generation system without speed sensor," in Applied Power Electronics Conference and Exposition (APEC), Charlotte, NC, 2015.

[10] Z. Zhang, Y. Zhao, W. Qiao and L. Qu, "A Space-Vector-Modulated Sensorless Direct-Torque Control for Direct-Drive PMSG Wind Turbines," IEEE Transactions on Industry Applications, vol. 50, no. 4, pp. 2331 - 2341, 2014.

[11] W. Hu, Y. Wang, X. Song and Z. Wang, "A Novel Sensorless Unity Power Factor Control Method for Six-phase PMSG in Direct Drive Wind Energy Conversion Systems," in Applied Power Electronics Conference and Exposition, 2009. APEC 2009, Washington, DC, 2009.

[12] B. Wang, Y. Zhao, Y. Yu, G. Wang, D. Xu and Z. Dong, "Speed-Sensorless Induction Machine Control in the Field-Weakening Region Using Discrete Speed-Adaptive Full-Order Observer," IEEE Transactions on Power Electronics, vol. 31, no. 8, pp. 5759 - 5773, 2016.

[13] Q. Huang and Z. Pan, "Sensorless control of permanent magnet synchronous generator in direct-drive wind power system," in International Conference on Electrical Machines and Systems (ICEMS), Beijing, 2011.

[14] E. Maldonado, C. Silva and M. Olivares, "Sensorless control of a doubly fed induction machine based on an Extended Kalman Filter," in Proceedings of the 2011-14th European Conference on Power Electronics and Applications (EPE 2011), Birmingham, 2011.

[15] I. Perez, J. Silva, E. Yuz and R. Carrasco, "Experimental sensorless vector control performance of a DFIG based on an extended Kalman filter," in 38th Annual Conference on IEEE Industrial Electronics Society, Montreal, QC, 2012.

[16] G. Rigatos, P. Siano and N. Zervos, "PMSG sensorless control with the use of the derivative-free nonlinear Kalman filter," in International Conference on Clean Electrical Power (ICCEP), Alghero, 2013.

[17] G. Rigatos, P. Siano and N. Zervos, "Sensorless Control of Distributed Power Generators With the Derivative-Free Nonlinear Kalman Filter," IEEE Transactions on Industrial Electronics, vol. 61, no. 11, pp. 6369 - 6382, 2014.

[18] M. Rizo, A. Rodriguez, E. Bueno and F. Rodriguez, "Robustness analysis of Wind Turbines based on PMSG with sensorless vector control," in 36th Annual Conference on IEEE Industrial Electronics Society, Glendale, AZ, 2010.

[19] V. Kordic, Kalman Filter, InTech, 2010.

[20] J. Brahmi, L. Krichen and A. Ouali, "Sensorless control of PMSG in WECS using artificial neural network," in 6th International Multi-Conference on Systems, Signals and Devices, 2009. SSD '09., Djerba, 2009.

[21] M. Singh and A. Chandra, "Application of Adaptive Network-Based Fuzzy Inference System for Sensorless Control of PMSG-Based Wind Turbine With Nonlinear-Load-Compensation Capabilities.pdf," IEEE Transactions on Power Electronics, vol. 26, no. 1, pp. 165 - 175, 2010.

[22] D. Aguilar, I. Candela, R. Munoz-Aguilar and A. Luna, "Sensorless control of PMSG-based wind Energy Conversion Systems using a FLL-based synchronization technique," in IECON 2011 - 37th Annual Conference on IEEE Industrial Electronics Society, Melbourne, VIC, 2011.

[23] A. El Magri, F. Giri, A. Abouloifa and A. El Fadili, "Sensorless adaptive observer of wind synchronous generator," in American Control Conference (ACC), Baltimore, MD, 2010.

[24] S. Fan, P. Wang and C. Wen, "A new sensorless control strategy used in direct-drive PMSG wind power system," in 2nd IEEE International Symposium on Power Electronics for Distributed Generation Systems (PEDG), Hefei, China, 2010.

[25] K. Gogas, G. Joos, B. Ooi and Y. Zhang, "Design of a Robust Speed and Position Sensorless Decoupled P-Q Controlled Doubly-Fed Induction Generator for Variable-Speed Wind Energy Applications," in Electrical Power Conference, Montreal, Que., 2007.

[26] M. Kutijaa, D. Suminaa and I. Čolović, "Magnetization of speed sensorless squirrel-cage induction generator for wind power application using a phase-locked loop," Electric Power Systems Research, vol. 122, p. 119–129, 2015.

[27] G. Marques and D. Sousa, "A DFIG sensorless method for direct estimation of slip position," in International Conference on Computational Technologies in Electrical and Electronics Engineering (SIBIRCON), Listvyanka, 2010.

[28] B. Mwinyiwiwa, Y. Zhang, B. Shen and B.-T. Ooi, "Rotor Position Phase-Locked Loop for Decoupled P-Q Control of DFIG for Wind Power Generation," IEEE Transactions on Energy Conversion, vol. 24, no. 3, pp. 758 - 765, 2009.

[29] N. Orlando, M. Liserre, V. Monopoli and A. Dell'Aquila, "Speed sensorless control of a PMSG for small wind turbine systems," in IEEE International Symposium on Industrial Electronics, Seoul, 2009.

[30] S. Yang, X. Zhang, C. Zhang and Z. Xie, "Sensorless control for PMSG in direct-drive wind turbines," in 2nd IEEE International Symposium on Power Electronics for Distributed Generation Systems (PEDG), Hefei, China, 2010.

[31] J. Liu, H. Nian, J. Li and R. Zeng, "Sensorless control of PMSG for wind turbines based on the on-line parameter identification," in International Conference on Electrical Machines and Systems, 2009. ICEMS 2009. , Tokyo, 2009.

[32] M. Fatu, C. Lascu, G. Andreescu and R. Teodorescu, "Voltage Sags Ride-Through of Motion Sensorless Controlled PMSG for Wind Turbines," in Industry Applications Conference, 42nd IAS Annual Meeting, New Orleans, LA, 2007.

[33] T. Senjyu, S. Tamaki, N. Urasaki and K. Uezato, "Wind velocity and position sensorless operation for PMSG wind generator," in The Fifth International Conference onPower Electronics and Drive Systems, 2003.

[34] [34] L. Xu and W. Cheng, "Torque and reactive power control of a doubly fed induction machine by position sensorless scheme," IEEE

Transactions on Industry Applications, vol. 31, no. 3, pp. 636 - 642, 1995.

[35] P. Vas, Sensorless Vector and Direct Torque Control (Monographs in Electrical and Electronic Engineering), Oxford University Press, July 9, 1998.

[36] N. T. Hai, S.-H. Jang, H.-G. Park and D.-C. Lee, "Sensorless control of PM synchronous generators for micro wind turbines," in Power and Energy Conference, 2008. PECon 2008. IEEE 2nd International, Johor Bahru.

[37] T. Senjyu, Y. Ochi, E. Muhando and N. Urasaki, "Speed and Position Sensor-less Maximum Power Point Tracking Control for Wind Generation System with Squirrel Cage Induction Generator," in Power Systems Conference and Exposition, 2006. PSCE '06. 2006 IEEE PES, Atlanta, GA.

[38] R. Cardenas, R. Pena, J. Clare and G. Asher, "MRAS Observers for Sensorless Control of Doubly-Fed Induction Generators," IEEE Transactions on Power Electronics, vol. 23, no. 3, pp. 1075 - 1084, 2008.

[39] H.-C. Tseng and S. Cheng, "Robust sensorless control of PMSG with MRAS in variable speed wind energy conversion system," in International Conference on Mechatronics and Automation (ICMA), 2011, Beijing.

[40] K. Huang, W. Li, S. Huang and L. Xiao, "Sensorless control of direct-driven permanent magnet wind power generation system based on improved MRAS," in International Conference on Electrical Machines and Systems (ICEMS), Beijing, 2011.

[41] M. Carmeli, F. Castelli-Dezza, M. Iacchetti and R. Perini, "Effects of Mismatched Parameters in MRAS Sensorless Doubly Fed Induction Machine Drives," IEEE Transactions on Power Electronics, vol. 25, no. 11, pp. 2842 - 2851, 2010.

[42] M. Pattnaik and D. Kastha, "Adaptive Speed Observer for a Stand-Alone Doubly Fed Induction Generator Feeding Nonlinear and Unbalanced Loads," IEEE Transactions on Energy Conversion, vol. 27, no. 4, pp. 1018 - 1026, 2012.

[43] R. Pena, R. Cardenas, J. Proboste and G. Asher, "Sensorless Control of Doubly-Fed Induction Generators Using a Rotor-Current-Based MRAS Observer," IEEE Transactions on Industrial Electronics, vol. 55, no. 1, pp. 330 - 339, 2008.

[44] G. Marques, V. Pires, S. Sousa and D. Sousa, "Evaluation of a DFIG rotor position-sensorless detector based on a hysteresis controller," in International Conference on Power Engineering, Energy and Electrical Drives, 2009. POWERENG '09., Lisbon, 2009.

[45] M. Pattnaik and D. Kastha, "Harmonic Compensation With Zero-Sequence Load Voltage Control in a Speed-Sensorless DFIG-Based Stand-Alone VSCF Generating System," IEEE Transactions on Industrial Electronics, vol. 60, no. 12, pp. 5506 - 5514, 2013.

[46] R. Cardenas, R. Pena, J. Proboste and G. Asher, "MRAS observer for sensorless control of standalone doubly fed induction generators," IEEE Transactions on Energy Conversion, vol. 20, no. 4, pp. 710-718, 2005.

[47] Y. Guofeng, L. Yongdong, C. Jianyun and J. Xinjian, "A novel position sensor-less control scheme of Doubly Fed Induction Wind Generator based on MRAS method," in Power Electronics Specialists Conference, Rhodes, 2008.

[48] J. Hu, W. Zhang, H. Wang and Y. He, "Improved MRAS observer and sensorless control of DFIG during network voltage unbalance," in IEEE International Electric Machines and Drives Conference, Miami, FL, 2009.

[49] W. Liu, L. Chen, J. Ou and S. Cheng, "Simulation of PMSG wind turbine system with sensor-less control technology based on model reference adaptive system," in International Conference on Electrical Machines and Systems (ICEMS), Beijing, 2011.

[50] G. Marques and D. Sousa, "New Sensorless Rotor Position Estimator of a DFIG Based on Torque Calculations—Stability Study," IEEE Transactions on Energy Conversion, vol. 27, no. 1, pp. 196 - 203, 2011.

[51] M. Pattnaik and D. Kastha, "Comparison of MRAS based speed estimation methods for a stand alone Doubly Fed Induction Generator," in International Conference on Energy, Automation, and Signal (ICEAS), 2011, Bhubaneswar, Odisha.

[52] I. Serban, G. Andreescu, L. Tutelea and C. Lascu, "New State Observers and Sensorless Control of Wound Rotor Induction Generator (WRIG) at Power Grid with Experimental Characterization," in 32nd Annual Conference on IEEE Industrial Electronics, Paris, 2006.

[53] X. Hao, C. W. Zhang and X. Zhang, "A Comparision of Sensorless Control Strategies of Doubly Fed Induction Generator," in International Conference on Energy and Environment Technology, Guilin, Guangxi, 2009.

[54] A. Consoli, G. Scarcella and A. Testa, "Industry application of zero-speed sensorless control techniques for PM synchronous motors," IEEE Transactions on Industry Applications, vol. 37, no. 2, pp. 513 - 521, 2001.

[55] D. Diaz Reigosa, F. Briz, C. Blanco Charro and A. Di Gioia, "Sensorless Control of Doubly Fed Induction Generators Based on Rotor High-Frequency Signal Injection," IEEE Transactions on Industry Applications, vol. 49, no. 6, pp. 2593 - 2601, 2013.

[56] D. Saltiveri, A. Arias, G. Asher, M. Sumner, P. Wheeler, L. Empringham and C. Silva, "Sensorless Control of Surface Mounted Permanent Magnet Synchronous Motors Using Matrix Converters,"

Electrical Power Quality and Utilisation, vol. 21, no. 1, pp. 59-67, 2006.

[57] G. Xie, K. Lu, S. K. Dwivedi, J. R. Rosholm and F. Blaabjerg, "Minimum-Voltage Vector Injection Method for Sensorless Control of PMSM for Low-Speed Operations," IEEE Transactions on Power Electronics, vol. 31, no. 2, pp. 1785 - 1794, 2016.

[58] Q. Tang, A. Shen, X. Luo and j. xu, "PMSM Sensorless Control by Injecting HF Pulsating Carrier Signal into ABC Frame," IEEE Transactions on Power Electronics, 2016.

[59] Z. Zhu, A. Almarhoon and P. Xu, "Improved Rotor Position Estimation Accuracy by Rotating Carrier Signal Injection Utilizing Zero-Sequence Carrier Voltage for Dual Three-Phase PMSM," IEEE Transactions on Industrial Electronics, 2016.

[60] P. L. Xu and Z. Zhu, "Novel Square-Wave Signal Injection Method Using Zero Sequence Voltage for Sensorless Control of PMSM Drives," IEEE Transactions on Industrial Electronics, 2016.

[61] Y. Iwaji, R. Takahata, T. Suzuki and S. Aoyagi, "Position sensorless control method at zero speed region for permanent magnet synchronous motors using the neutral point voltage of stator windings," in Energy Conversion Congress and Exposition (ECCE), 2014.

[62] S.-I. Kim, J.-H. Im, E.-Y. Song and R.-Y. Kim, "A New Rotor Position Estimation Method of IPMSM Using All-Pass Filter on High-Frequency Rotating Voltage Signal Injection," IEEE Transactions on Industrial Electronics, vol. 63, no. 10, pp. 6499 - 6509, 2016.

[63] X. Fei, W. Hao-xiong, C. Min-liang and L. Yong, "A novel sensorless control of PMSG based on sliding mode observer," in XIX International Conference on Electrical Machines (ICEM), Rome, 2010.

[64] J. A. Cortajarenaa and J. D. Marcos, "Neural Network Model Reference Adaptive System Speed Estimation for Sensorless Control of a Doubly Fed Induction Generator," Electric Power Components and Systems, vol. 41, no. 12, pp. 1146-1158, 2013.

[65] L. Lan and L. Yanli, "Rotor Speed Identification of Doubly-Fed Generator System Based on Neural Network," in International Conference on E-Learning, E-Business, Enterprise Information Systems, and E-Government, Hong Kong, 2009.

[66] X. Hao, C. W. Zhang, X. Zhang and Y. Yu, "A Novel Sensorless Control Strategy of Doubly Fed Induction Generator Based on Stator Voltage," in Power and Energy Engineering Conference (APPEEC), Chengdu, 2010.

[67] G. Marques and D. Sousa, "Air-Gap-Power-Vector-Based Sensorless Method for DFIG Control Without Flux Estimator," IEEE Transactions on Industrial Electronics, vol. 58, no. 10, pp. 4717 - 4726, 2011.

[68] E. Koutroulis and K. Kalaitzakis, "Design of a Maximum Power Tracking System forWind-Energy Conversion Applications," IEEE Transactions on Industrial Electronics, vol. 53, no. 2, pp. 486 - 494, 2006.

[69] M. Messaoud and A. Rachid, "Comparative study of a small size wind generation system efficiency for battery charging," Serbian Journal of Electrical Engineering, vol. 10, no. 2, pp. 261-274, 2013.

[70] W. Kramer, S. Chakraborty, B. Kroposki and H. Thomas, Advanced power electronic interfaces for distributed energy systems, Cambridge: National Renewable Energy Laboratory(NREL), 2008.